

## Nonequilibrium dynamics in a three-dimensional spin glass

T. Jonsson, K. Jonason, P. Jönsson, and P. Nordblad

*Department of Materials Science, Uppsala University, Box 534, SE-751 21 Uppsala, Sweden*

(Received 27 August 1998)

Nonequilibrium dynamics in a Ag(11%Mn) spin glass has been studied by low frequency ac-susceptibility and magnetic relaxation experiments. The results unequivocally show that spin structures that memorize the cooling process are imprinted in the system. These imprinted structures disclose themselves through dramatic changes of the dynamics on reheating the spin glass through the temperatures where intermittent halts or changes of the cooling rate have been imposed. We can qualitatively interpret our results in terms of a real space picture based upon spin-glass domains, droplet excitations and chaos. [S0163-1829(99)03813-8]

### I. INTRODUCTION

A successful real space theory for the dynamics of three-dimensional spin-glass systems is the droplet model developed a decade ago by Fisher and Huse.<sup>1</sup> Particular experimental characteristics such as the aging phenomenon<sup>2</sup> and the nonexistence of a phase transition in a magnetic field<sup>3</sup> are inherent properties of the droplet spin-glass model. However, the validity of this model has been questioned: e.g., a compact domain growth picture is not consistent with the multiple memory effect recently found in three-dimensional spin-glass systems.<sup>4,5</sup> Figure 1 shows a low frequency ac-susceptibility experiment on a Cu(Mn) spin glass where this suggestive effect is illustrated. In this paper, extended measurements of some associated nonequilibrium features of the ac susceptibility and the dc-magnetic relaxation on the three-dimensional spin-glass material Ag(11 at.% Mn) are presented. The results can qualitatively be understood in terms of a real space picture employing spin glass domains and chaos and disperse droplet excitations to explain the history dependence of the magnetization process. We do not try to interpret these results on memory and aging in spin glasses in terms of non-real-space models.<sup>6</sup>

### II. THE DROPLET MODEL

The results of this study are interpreted in the spirit of the droplet model<sup>1</sup> using relevant parts as summarized in the following points.

(i) A spin-glass equilibrium state is unique but two-fold degenerate by its spin reversal symmetric state.

(ii) Chaos with temperature—a small temperature shift changes the spin configuration of the equilibrium state completely on long enough length scales.<sup>7</sup>

(iii) The length scale  $l$  up to which no essential change in spin configuration is observed after a temperature change  $\Delta T_*$  introduces the concept of an overlap length  $l(\Delta T_*)$ .

(iv) In the nonequilibrium case, the development towards the ground state is governed by the growth of domains belonging to either of the two degenerate equilibrium states. The typical domain size after a time  $t_w$  at a constant temperature  $T$  is

$$R \propto \left( \frac{T \ln(t_w / \tau_0)}{\Delta(T)} \right)^{1/\psi}, \quad (1)$$

where  $\tau_0$  is a microscopic time of order  $10^{-13}$ s.  $\Delta(T)$  sets the free energy scale and  $\psi$  is a barrier exponent. This length scale  $R$ , that we often will refer to as a typical domain size, should not be taken literally, but rather be considered as a typical measure of the smallest separation between domain walls after the wait time  $t_w$ .

In order to discuss the relaxation towards equilibrium, a three-dimensional Ising spin-glass quenched to a temperature  $T_1 < T_g$  is considered. The state at  $t=0$  is hence characterized by spins of random direction. To further simplify the following argumentation it is also assumed that the spins are situated on a regular lattice. In the droplet model there exists only two degenerate equilibrium configurations,  $\Psi$  and its spin reversal counterpart  $\tilde{\Psi}$ , it is thus possible to map all spins to either of the two desired equilibrium configurations immediately after a quench. Citing Fisher and Huse<sup>1</sup> “This results in an interpenetrating network of regions of the two states.” In fact, the domain walls of one lattice spacing,

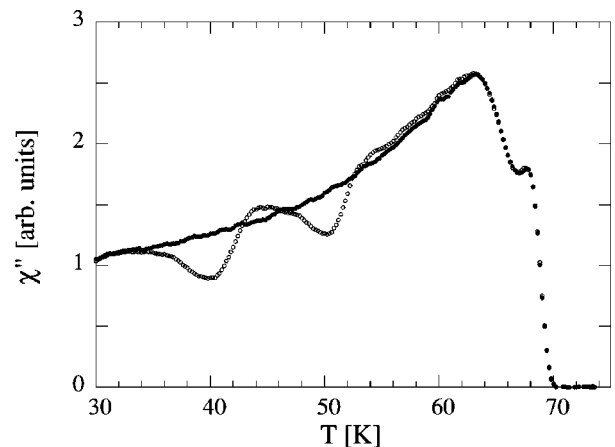


FIG. 1. The out-of-phase component of the ac susceptibility of a Cu(13.5 at% Mn) ( $T_g \approx 68$  K) spin glass measured on continuous heating after the sample has been subjected to two intermittent stops of order  $10^4$  s at 40 and 50 K during the cooling procedure. The two pronounced dips in the curve occur at the temperatures of the stops at constant temperature during cooling.  $f = 1.7$  Hz.

which separates the two states  $\Psi$  and  $\tilde{\Psi}$  at  $t=0$  after the quench should have a fractal surface giving rise to fractal domains of many sizes (see the critical fractal cluster model suggested some 15 years ago by Malozemoff and Barbara<sup>8</sup>). The subsequent equilibration process at  $t>0$  is governed by droplet excitations yielding a domain growth to a typical length scale which depends on temperature and wait time  $t_{w1}$  according to Eq. (1). After this time, fractal structures typically smaller than  $R(T_1, t_{w1})$  have become equilibrated. One implication of this argument is that relevant changes of the spin configuration only occur in disperse regions and on short length scales whereas spin structures on large length scales are virtually unaffected after the wait time  $t_{w1}$ . If the system thereafter is quenched to a considerably lower temperature  $T_2$ , a new fractal domain structure can be mapped onto the equilibrium configuration at  $T_2$ . The short length scale limit is now set by the overlap length  $l(T_1 - T_2)$  and fractal structures will be “washed out” with increasing wait time  $t_{w2}$  starting from this length scale and ending at the size  $R(T_2, t_{w2})$ . Structures on longer length scales are again intact. If the system is further quenched and then instantly reheated to  $T_2$ , the domain structure at  $T_2$  of course remains unaffected, but also, when instantaneously heated back to  $T_1$ , the restructuring on short length scales  $R(T_2, t_{w2}) \ll R(T_1, t_{w1})$  that occurred at  $T_2$  is rapidly washed out and the system is effectively left with only the large length scale domain structure which was imprinted during the original wait time at  $T_1$ . If the fractal droplet model is relevant, these basic properties of the logarithmically slow (eternal?) equilibration process should be reflected in the dynamic response of a real three-dimensional spin glass subjected to a corresponding thermal history. In a real experimental situation, the system can only be cooled and heated at a controlled but finite rate. The domain growth is in such processes governed by the cooling/heating rate and limited by an interplay between the domain growth [Eq. (1)], the chaotic nature of the spin-glass phase, and the overlap between states on short enough length scales. Accounting for this complication, we have designed a series of dynamic magnetization and susceptibility experiments that should mirror the discussed development of a domain structure in an equilibrating three-dimensional spin glass.

Droplet excitations occur on time limited length scales and are in fact responsible for the equilibration process of the quenched spin glass, also giving rise to the domain growth function Eq. (1). If a weak magnetic field is applied on the spin glass at time  $t_{\text{obs}}=0$ , the time-dependent response  $m(t_{\text{obs}})$  is due to a continuous magnetization process governed by polarization of droplets of size  $L(t_{\text{obs}})$

$$L \propto \left( \frac{T \ln(t_{\text{obs}}/\tau_0)}{\Delta(T)} \right)^{1/\psi}. \quad (2)$$

Since  $L$  grows with the same logarithmic rate as  $R$ , the relevant droplet excitations and the actual domain size become comparably large at time scales  $t_w \approx t_{\text{obs}}$ . For  $t_{\text{obs}} \ll t_w$  the relevant excitations occur mainly within equilibrated regions while for  $t_{\text{obs}} \gg t_w$  these excitations occur on length scales of the order of the growing domain size and yield a nonequilibrium response. A crossover occurs in the intermediate region  $t_w \approx t_{\text{obs}}$  which is characterized by a maximum in

the relaxation rate  $S(t) = 1/H \partial m(t) / \partial \log_{10} t$ . This aging behavior is also reflected in low frequency ac-susceptibility measurements. Different from dc-relaxation measurements is that the observation time is kept constant by the probing frequency  $\omega/2\pi$  according to  $t_{\text{obs}} = 1/\omega$  and hence, in an experiment at constant temperature, sets the associated probed length scale  $L(T, 1/\omega)$  fixed. In this study we are primarily interested in the processes that affect the response at the observation time of the experiment, the consequences of these are best exposed in plots of the relaxation rate  $S$  vs  $t_{\text{obs}}$  for different wait times or the out-of-phase component of the ac susceptibility vs time at constant temperature or vs temperature at different cooling and heating rates. Therefore, the dc-relaxation measurements are primarily presented in the form of the relaxation rate  $S$  and the ac susceptibility is represented by its imaginary part  $\chi''$  these quantities can be related through the relation<sup>9</sup>

$$\chi''(\omega) \approx \frac{\pi}{2} S(t_{\text{obs}}), \quad t_{\text{obs}} = 1/\omega. \quad (3)$$

### III. EXPERIMENTAL

The sample was prepared by melting pure Ag and Mn together at  $T = 1000^\circ\text{C}$  in an evacuated atmosphere. After annealing the sample at  $850^\circ\text{C}$  for 72 h it was water quenched to room temperature.

The experiments have been performed in a noncommercial low-field SQUID magnetometer.<sup>10</sup> The dc magnetic field is generated by a small superconducting solenoid always working in persistent mode during measurements. The ac field was generated by a copper coil directly wound on the sample which is shaped as a 5 mm long cylinder, 2.5 mm in diameter. The magnetic response of the sample, subtracted by the ac field from a compensating coil, was recorded with a set of pick-up loops positioned to form a third order gradiometer. At the position of the sample, the resulting rms value of the ac field was 0.1 Oe and the background field was less than 1 mOe. All ac-susceptibility measurements were performed at a frequency of 1.7 Hz. A sapphire rod was used to provide a good thermal contact between the heater, the thermometer and the sample.

### IV. RESULTS AND DISCUSSION

#### A. Aging characteristics

Figures 2 and 3 introduce the overall behavior of the dynamic susceptibility of our Ag(11 at. % Mn) sample and expose two classical manifestations of the aging phenomenon in spin glasses. In the inset to Fig. 2 both components of the ac susceptibility  $\chi(\omega) = \chi'(\omega) + i\chi''(\omega)$  at the frequency  $\omega/2\pi = 1.7$  Hz are plotted vs temperature at a cooling rate of 0.25 K/min. The maximum in  $\chi'(T)$ , defining the freezing temperature, is accompanied by the onset of an out-of-phase component of the susceptibility. In the main frame of Fig. 2 the influence of aging on  $\chi''$  is illustrated by a plot of  $\chi''$  vs time elapsed at 23 K, where the continuous cooling was interrupted. Figure 3 exemplifies the results from an ordinary zero field cooled (ZFC) aging experiment at  $T_m = 27$  K, in (a) the magnetization and in (b) the corresponding relaxation rate is plotted vs the observation time. The

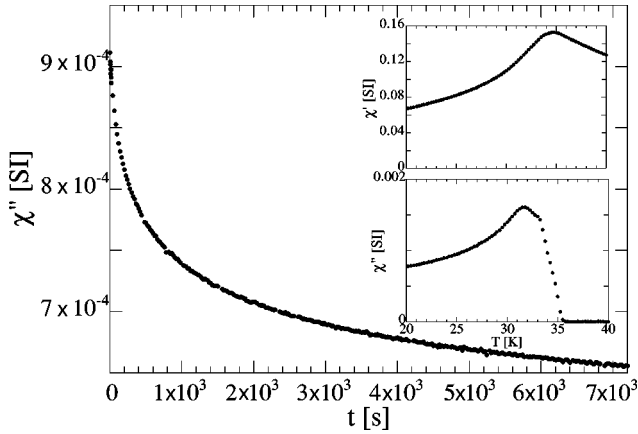


FIG. 2. Relaxation of  $\chi''(t)$  with time at constant temperature after the sample has been cooled from a temperature above  $T_g$  to  $T=23$  K. Inset: both components of the ac susceptibility vs  $T$  measured at a cooling rate of 0.25 K/min.  $f=1.7$  Hz,  $h_{ac}=0.1$  Oe, Ag(11 at. % Mn).

sample is probed in a dc field of 1 Oe after the wait times  $t_w=100$  s (open symbols) and  $t_w=3000$  s (filled symbols) at  $T_m$ . The signatures of aging in spin glasses: an inflection point in  $m(t)$  and a corresponding maximum in  $S(t)$  vs  $\ln t_{obs}$  are reproduced in the figure.

Some words about time and nonequilibrium dynamics are in order. Experimentally we are confined to time scales set by the cooling and heating rates and the time it takes to thermally equilibrate the sample to a constant temperature. Although spin-glass dynamics occurs on all time scales rang-

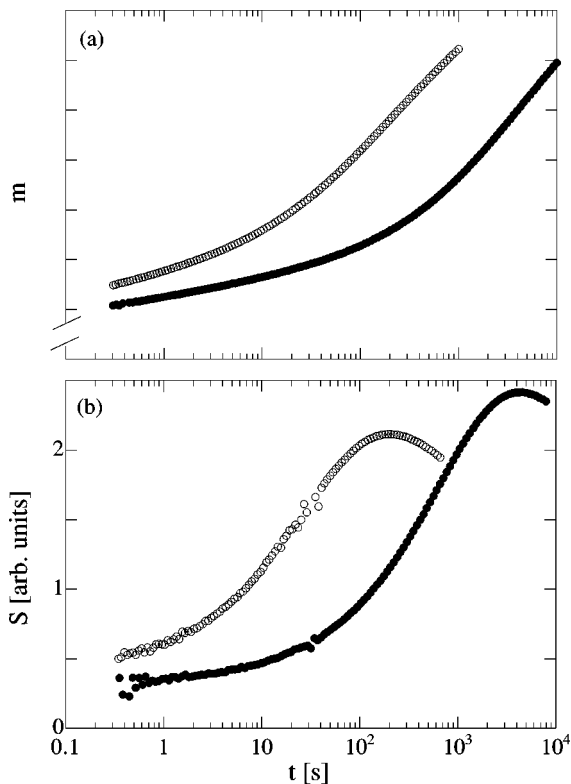


FIG. 3. Zero field cooled magnetization vs observation time at 23 K. (a)  $m(t)$  vs  $\ln t$  (b) relaxation rate  $S(t)$ .  $H_{dc}=1$  Oe, Ag(11 at. % Mn).

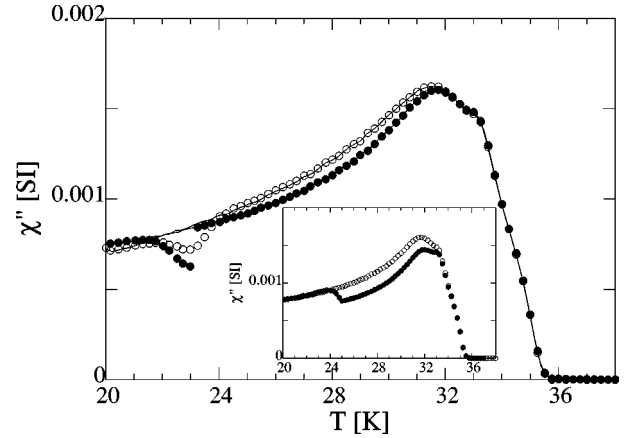


FIG. 4.  $\chi''(T)$  vs  $T$  measured on cooling (solid circles) and heating (open circles) at a rate of 0.25 K/min. The sample was intermittently kept at  $T=23$  K for  $t_w=7200$  s during cooling. Solid lines show the corresponding curves without the interrupted cooling at 23 K. The inset shows  $\chi''(T)$  using two different cooling rates: 0.25 K/min (open circles) and 0.005 K/min (solid circles). The slow cooling rate is changed to 0.25 K/min at 25 K.  $f=1.7$  Hz,  $h_{ac}=0.1$  Oe, Ag(11 at. % Mn).

ing from  $10^{-13}$  s to infinity, the shortest observation times where consequences of nonequilibrium dynamics can be observed experimentally are confined to  $t_{obs} \geq 10^{-3} t_{aef}$  where  $t_{aef}$  is an effective age of the system set by the cooling and heating rate or the time spent at constant temperature. That is, when  $t_{obs} \ll t_{aef}$  no aging is observed and the dynamic response of the system appears stationary. In practice this applies to most ac-susceptibility measurements at frequencies larger than 20 Hz ( $t_{obs}=1/\omega \approx 10^{-2}$  s). On the other hand, in a dc magnetic relaxation experiment spanning some decades in time, the observation time of the experiment continuously increases and  $\ln t_{obs}$  unavoidably approaches  $\ln t_{aef}$  at long enough observation times and effects of the aging process becomes discernible. The different times necessary to discuss the aging behavior are related according to  $t_{aef} \approx t_w + t_{obs} = t_a$ , where  $t_a$  is the total time spent at constant temperature, i.e., the age of the system.

We will continue by discussing results from ac-susceptibility experiments using different cooling rates and employing intermittent stops at different temperatures during the cooling of the sample, and interpret this cooling behavior as well as the subsequent heating curves (always recorded at one and the same heating rate) in terms of an assumed domain structure imprinted during cooling. This discussion will be complemented by results from dc-magnetic relaxation experiments subsequent to cooling and heating procedures that closely mimic those of the ac experiments.

### B. ac susceptibility: Cooling rate dependence and memory

A simple memory effect in the low frequency ac-susceptibility is shown in Fig. 4 after the following sequence has been performed. The sample is cooled to 23 K while measuring every 0.25 K (filled circles). At 23 K the sample is subjected to a wait time  $t_w=7200$  s during which  $\chi''$  decays (see Fig. 3). After this wait time, the sample is further cooled to 20 K and then immediately reheated, the data on heating are indicated by open circles in the figure. Both the

cooling and the heating is made with the same rate 0.25 K/min. The results from identical cooling and a heating procedures, but without the wait time at 23 K, are indicated by the full lines in Fig. 4 for reference. The effect of the relaxation during the wait time is clearly visible in the cooling curve as a dip in  $\chi''(T)$ , followed by a rather rapid increase and approach to the reference curve at temperatures below 23 K on the continued cooling and, as expected from the described droplet model, it also reappears as a corresponding dip in  $\chi''(T)$  centered around  $T=23$  K in the heating curve. The merging with the cooling reference curve on continued cooling can be interpreted as an effect of chaos with temperature<sup>7</sup> and a region of overlapping states  $\Delta T_*$ . The dip on reheating is a consequence of the imprinted spin configuration at  $T=23$  K on large length scales. That is, when returning to this temperature all domain growth at lower temperatures have occurred on length scales  $\ll R(23 \text{ K}, 7200 \text{ s})$  and these are here washed out on shorter time scales leaving a system with an effectively equivalent domain configuration to the one originally obtained during the wait time at  $T=23$  K.

An immediate consequence of the chaos and overlap concepts is that the ac susceptibility depends on the cooling rate. Larger domains have time to grow within the overlap region  $\Delta T_*$  when cooling the spin glass at a slower rate. Thus, the observed magnitude of  $\chi''(T)$  will be closer to the equilibrium level in a slow cooling process than in a fast. This prediction is confirmed in the inset to Fig. 4, where  $\chi''(T)$  at two different cooling rates 0.25 and 0.005 K/min are shown. The overlap concept is further supported by the fact that when suddenly at 25 K the cooling rate is increased from 0.005 to 0.25 K/min, the cooling curve within a distance of  $\Delta T_* \approx 1$  K merges with the fast cooling curve. Assuming that the domain size,  $R(T, t_c)$ , at all temperatures in the cooling process is limited by a characteristic time  $t_c$ , which is set by the cooling rate and an interplay between chaos and the overlap length, obviously this time  $t_c$  must increase with decreasing cooling rate. In the  $\chi''(T)$  experiments, droplet excitations on the length scale  $L(T, 1/\omega)$  govern the response, these excitations include a large amount on the size of the domains if  $1/\omega$  is of order  $t_c$ , but such domain sizes progressively become rare with an increasing  $t_c$ . This implies as mentioned above that the measured susceptibility decreases with decreasing cooling rate and that a change of the cooling rate must result in a crossover from one cooling rate characteristic curve to the other. It is of course also possible to cross from the fast to the slow cooling curve in a similar way.

Regarding the two reference curves, measured at 0.25 K/min, in the main frame of Fig. 4, it may be argued that they should be almost identical,<sup>4</sup> since a domain structure on continuously decreasing long length scales  $R(T, t_c)$  is imprinted in the system on cooling the sample. This structure should then also govern the ac susceptibility on reheating the sample at the same rate. However, as is seen in the figure, the two curves differ notably in magnitude. Two main factors can explain the deviation. Firstly, the effective heating time scale  $t_h$  is different from the cooling time  $t_c$ , although the rates are the same, 0.25 K/min. This difference can be understood considering the existence of an overlap length and the fact that the domain growth or, equivalently, the domain

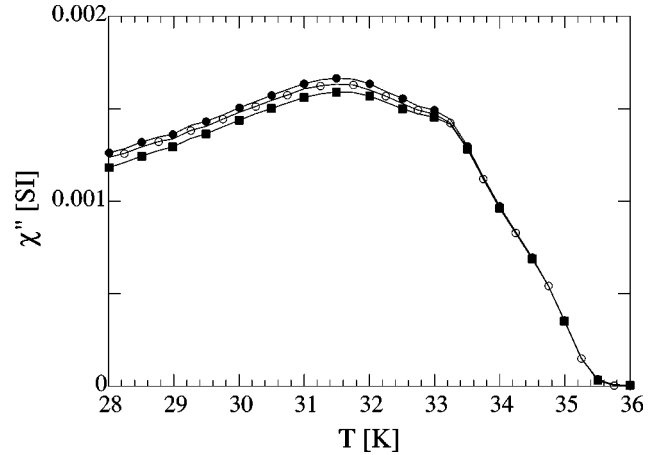


FIG. 5.  $\chi''(T)$  measured on heating at a rate of 0.25 K/min. The different curves are recorded after cooling the sample at different cooling rates: 0.005 K/min (solid squares), 0.25 K/min (open circles), and 4 K/min (solid circles).  $f=1.7$  Hz,  $h_{ac}=0.1$  Oe, Ag(11 at. % Mn).

wall movements are faster at higher temperatures. At any subsequent temperature  $T$  on a cooling or heating process, overlapping equilibrium state configurations have already been created at nearby temperatures within  $T \pm \Delta T_*$ . Hence, the domains have grown to a larger size when reaching  $T$  in cooling and a smaller size on heating, which in terms of time implies  $t_c > t_h$ . If the mapping was perfect, so that the domain structure on long length scales was fully intact on reheating, the heating curve would still coincide with the cooling curve as long as  $t_h < t_c$ , since we would probe an identical undisturbed domain structure determined by  $R(T, t_c) [ > R(T, t_h) ]$  at all temperatures. However, secondly, there is a reinitialization of the gained domain structure on length scales that do not overlap with the created domains at a lower temperature in a continuous cooling process. This implies that the domain structure on reheating the sample has become partially reconstructed also on length scales of order  $R(T, t_c)$ , i.e., the system appears less equilibrated and the susceptibility attains a comparably larger magnitude. The behavior on changing from cooling to heating the sample requires a comment. In Fig. 4 this change occurs at  $T=20$  K resulting in a heating reference curve which initially is smaller in magnitude than the cooling reference curve. This is explained by the fact that the sample spends the longest time in the temperature interval within the overlap region  $(20 \text{ K} + \Delta T_*) \pm \Delta T_*$  first during cooling and then in the subsequent heating.

To elaborate further on the cooling and heating rate dependence, we show in Fig. 5 three curves obtained at one and the same heating rate, but recorded after cooling the sample at 4, 0.25, and 0.005 K/min. The differences between the curves are significant and in accord with the discussion above that a domain structure on long length scales  $R(T, t_c)$  is imprinted but also reinitialized during continuous cooling. We thus expect that the curve recorded at a cooling rate of 4 K/min should always yield  $t_h > t_c$  and the system should appear least equilibrated and have the largest magnitude of  $\chi''(T)$ . The curve obtained after cooling at 0.005 K/min has an imprinted spin structure characterized by  $t_c \gg t_h$  and  $\chi''(T)$  should have a substantially smaller magnitude. The

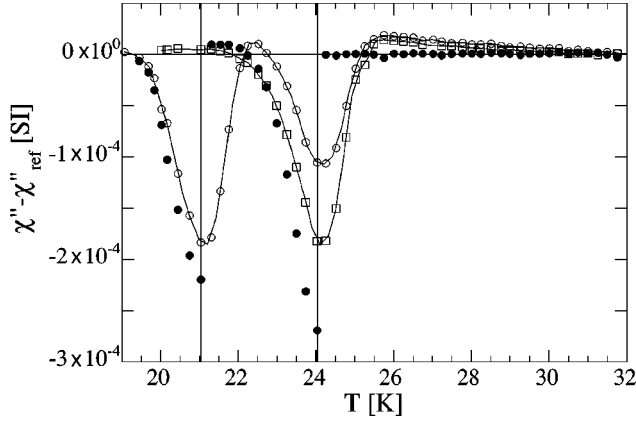


FIG. 6.  $\chi''(T) - \chi''_{\text{ref}}(T)$  vs  $T$ , measured at a cooling (solid symbols) or heating rate (open symbols) of 0.25 K/min. The sample was kept 30 000 s at 24 and at 21 K during cooling. The open squares indicate an experiment where the sample only was kept 30 000 s at 24 K during cooling.  $f = 1.7$  Hz,  $h_{\text{ac}} = 0.1$  Oe, Ag(11 at. % Mn).

curve measured after cooling at 0.25 K/min is expected to be found in between the other two, just as is seen in the figure.

For visual clarity in the following figures, all presented ac-susceptibility data are subtracted by either the cooling or the heating reference curve. These two reference curves are obtained using a cooling and heating rate of 0.25 K/min (see Fig. 4). Since the ac susceptibility always decreases towards the equilibrium value when the system ages at constant temperature, data points which are positive in such plots indicate a state further away from equilibrium than the corresponding points on the reference curve. For negative values the data points are closer to equilibrium. Furthermore, in all these experiments, the dc field is zero and the cooling is always initiated at  $T = 40$  K where the system is paramagnetic.

As has been experimentally observed in a recent study on memory effects in spin glasses<sup>5</sup> and was reproduced in Fig. 1, the single memory experiment presented in Fig. 4 can be extended to include two (or more) wait times at well separated temperatures during the cooling of the sample. A procedure, which in the subsequent heating process results in dips in the ac susceptibility positioned at each of these temperatures. For our current sample, this intriguing behavior is illustrated in Fig. 6 where the sample has been subjected to two wait times of 30 000 s duration, first at  $T = 24$  K and then at  $T = 21$  K. Except at these particular temperatures the sample is cooled and heated with the usual rate of 0.25 K/min. As can be seen from the open circles in Fig. 6, the equilibration at each temperature gives rise to corresponding dips when reheating the sample.

Evidently from the results discussed above, it is possible to imprint a spin configuration at a temperature where the spin glass has been allowed to age and recover this state when returning to the same temperature, and even to imprint and recover two or more equilibrated spin configurations at well separated temperatures. This ability excludes, as pointed out recently,<sup>5</sup> that new compact domains grow at each aging temperature. In other words, assuming that  $|T_1 - T_2| > \Delta T_*$ , it is impossible to imagine that compact  $T_1$  domains coexist with compact  $T_2$  domains. However, by assuming that the equilibration process does not correspond to the growth of compact domains but rather, as discussed above, a

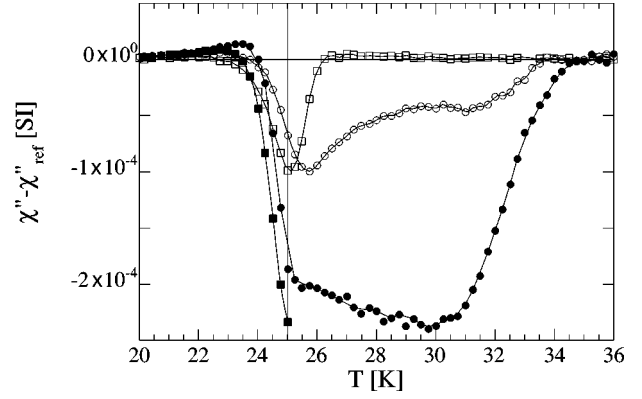


FIG. 7.  $\chi''(T) - \chi''_{\text{ref}}(T)$  vs  $T$ , measured on cooling at different rates (solid symbols) and heating (open symbols) at a rate of 0.25 K/min. Solid circles indicate a cooling process at 0.005 K/min down to 25 K, where the cooling rate is changed to 0.25 K/min. Open circles show the corresponding curve on heating at 0.25 K/min. Solid squares below 25 K show data after having kept the sample at 25 K for 7200 s using a cooling rate of 0.25 K/min and open squares the corresponding heating curve.  $f = 1.7$  Hz,  $h_{\text{ac}} = 0.1$  Oe, Ag(11 at. % Mn).

removal of fractal domain wall structures up to the length scale  $R$ , the results may still accord with the droplet model. To be more specific, the minimum length scale of the distance between domain walls, after the first wait time at  $T_1$  is typically  $R(T_1, t_{w1})$ . Chaos with temperature<sup>7</sup> implies that this structure is random at  $T_2$  on length scales larger than the overlap length  $l(T_1 - T_2)$ . After the wait time  $t_{w2}$  at  $T_2$  the domain wall movements have removed fractal structures on length scales up to  $R(T_2, t_{w2})$ . The spin configuration of the system can now be mapped on the equilibrium configurations at  $T_2$  and at  $T_1$ . The map at  $T_2$  yields an equilibrium system on length scales smaller than  $R(T_2, t_{w2})$  and a random system on larger length scales. The map at  $T_1$  on the other hand shows random structures on length scales between  $l(T_1 - T_2)$  and  $R(T_2, t_{w2})$  and on length scales larger than  $R(T_1, t_{w1})$ . In the real experiment, the configurations are less well defined and how well they are preserved in the thermal procedure depends on the length of the wait times, the cooling and heating rates and the separation between the temperatures  $T_1$  and  $T_2$ . On reheating the sample, the relative depth of the recovered dips in  $\chi''(T)$  in Fig. 6 mirrors how these structures have been preserved. For comparison, the ac susceptibility on heating the sample from 20 K after waiting  $t_w = 30\,000$  s only at  $T = 24$  K during the cooling, is included as squares in Fig. 6. Since this single memory dip is deeper than the corresponding double memory dip it can be concluded that during the wait time at  $T = 21$  K the first imprinted spin configuration at the preceding aging at  $T = 24$  K has been partly overwritten, i.e., the system has been partly reinitialized. It is also worth to notice that the relative depth of the dip on reheating the sample is temperature dependent; with increasing temperature, in otherwise identical single memory experiments, the dip becomes more and more shallow compared to the depth obtained during the original wait time at  $T_m$  on cooling (see also Fig. 7).

A partial reinitialization, is also evidenced from the positive values of the relative ac-susceptibility plotted in Fig. 6 a few K above and below the dip at 24 K, signaling an appar-

ently less equilibrated system as compared to the reference. Before discussing the origin of this behavior more thoroughly, it is advantageous to return to the very slow cooling experiment. In Fig. 7 the ac susceptibility during cooling with 0.005 K/min, subtracted by the corresponding data obtained with the cooling rate 0.25 K/min, is represented by filled circles. When passing the temperature  $T=25$  K the cooling rate is changed to 0.25 K/min resulting in a quick increase of the susceptibility towards the reference level. In fact it even crosses the reference curve during the preceding cooling to  $T=20$  K. The ac susceptibility of the subsequent heating, at rate 0.25 K/min, are shown by the open circles. As can be expected when considering the overlap length and a decrease of the reinitialization just when the cooling rate is increased, the system looks most equilibrated in a temperature interval  $T=(25 \text{ K} + \Delta T_*) \pm \Delta T_*$ . At higher temperatures, the spin configuration appears less equilibrated than the original slow cooling curve, but still closer to equilibrium than the reference heating curve (which is measured at the same heating rate, 0.25 K/min). This behavior mirrors both the continuously imprinted equilibrated spin configurations obtained during slow cooling and the simultaneous partial reinitialization of these configurations which occurs at lower temperatures. It must hence also be concluded that the equilibrated length scales  $R(T, t_c)$  obtained at each temperature in the slow cooling process are partly preserved during the whole experiment. For comparison we have in Fig. 7 included a single memory curve recorded at a cooling and heating rate of 0.25 K/min and waiting 7200 s at 25 K during cooling. Filled squares show the cooling curve and open squares the heating curve. It may be noticed that this dip is centered around  $T=25$  K as expected.

Figures 6 and 7 show that a long wait time at constant temperature also affects the ac-response at surrounding temperatures, so that the spin glass appears less equilibrated than in the reference procedure at temperatures separated more than  $\Delta T_*$  from the temperature where the aging took place. As discussed above, in the continuous cooling case the typical equilibrated domain size  $R(T, t_c)$  is governed by the effective cooling time  $t_c$ , which also sets an effective age and thus the magnitude of  $\chi''(T, t_c)$ . When the cooling is stopped at  $T_m$ , the domains can grow unrestricted, and after the wait time they have reached a size  $R(T_m, t_w)$ . When cooling is recaptured, this new domain size is adequate as long as the overlap length  $l(T_m - T) > R(T, t_w)$ , however, at temperatures just outside  $T \leq (T_m - \Delta T_*)$  the typical domain size is determined by the overlap length  $l(T_m - T) \ll R(T, t_w)$ . [The overlap length  $l(\Delta T)$  is a very rapidly decreasing function with  $\Delta T$ .] At lower temperatures, the cooling time again becomes the governing parameter. However, just outside the overlap region  $T_m - \Delta T_*$  the actual cooling time  $t_{ac}$  i.e., the time the sample has been kept within a region where the growing domain size overlaps with the domain size achieved at temperatures just above, is of course considerably shorter than the cooling time  $t_c$  of the continuous reference cooling procedure and thus  $R(T, t_{ac}) < R(T, t_c)$ . During the continued cooling,  $t_{ac}$  increases, but a temperature decrease at least of order  $\Delta T_*$  is needed to regain  $t_{ac} \approx t_c$  and a typical domain size equivalent to that of the continuous cooling procedure. These arguments suggest, in accord with the experiments, that the disturbed  $\chi''(T)$  curve at temperatures below  $T_m$  first

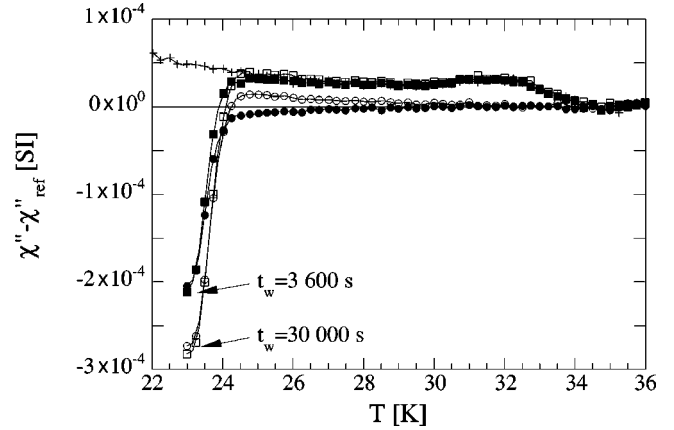


FIG. 8.  $\chi''(T) - \chi''_{ref}(T)$  vs  $T$ , measured on heating at 0.25 K/min, after the sample has been cooled to 23 K at 0.25 K/min (circles) or 4 K/min (squares) and kept at 23 K for 3600 s (solid symbols) or 30 000 s (open symbols). The pluses show a heating curve measured after cooling to the same temperature at 4 K/min without a stop at 23 K.  $f=1.7$  Hz,  $h_{ac}=0.1$  Oe, Ag(11 at. % Mn).

should increase towards and even cross the reference level as the temperature is decreased beyond  $\Delta T_*$ , go through a maximum deviation and then slowly approach  $\chi''_{ref}$  further away from  $T_m$ . Similar arguments as discussed above can also be applied to the heating curve at temperatures above  $T_m$ , i.e., the dip should be succeeded by a temperature region outside  $T_m + \Delta T_*$  where the relative susceptibility should become positive. The longer time the sample is kept at  $T_m$  the deeper the dip and the larger the positive levels outside the overlap region will become. This conclusion is further elucidated in an experiment where the sample is cooled, either with the rate 0.25 or 4 K/min, to the temperature 23 K where it is subjected to different wait times before it is heated with the rate 0.25 K/min. In Fig. 8 the ac susceptibilities, measured on heating, are indicated by filled symbols after the wait time  $t_w=3600$  s. Open symbols indicate the corresponding curves after a wait time  $t_w=30000$  s. To separate the two cooling rates, squares are used to symbolize the faster one while circles are used for the slower. Also included in Fig. 8 is a reference curve obtained during heating after cooling to 20 K with the fast rate 4 K/min. As can be seen, the system appears more reinitialized, at high enough temperatures, after a waiting time of 30 000 s. The effect is most pronounced in the case where a slow cooling rate was used. A wait time of 3600 s is apparently too short to realize a measurable reinitialization.

### C. Relaxation rate experiments

The usefulness of this fractal domain picture can be further examined by means of relaxation measurements where the observation time spans several decades. A zero-field-cooled relaxation experiment can be designed to give complementary information on the reinitialization observed in the ac susceptibility curves of Fig. 7. In these measurements, as in the ac experiments, the sample is cooled with a rate of 0.25 K/min to 23 K where it is subjected to a wait time  $t_w$ . The sample is then heated at the rate 0.25 K/min but only to 25 K where the sample is kept at constant temperature and after a time of 10 s a magnetic field of 1 Oe is

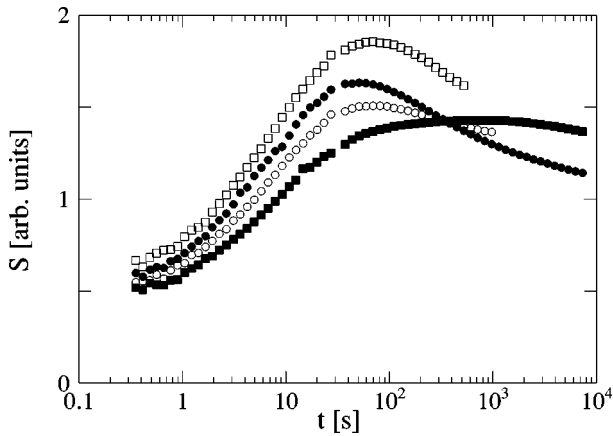


FIG. 9. Relaxation rate  $S$  vs  $\ln t$ , measured at 25 K after having cooled the sample at 0.25 K/min to 23 K and keeping it there a wait time  $t_w$  before re-heating it to 25 K and applying the dc field after 10 s at constant temperature.  $t_w=0$  (filled squares), 3600 s (open circles), and 30 000 s (filled circles). A reference curve measured after cooling the sample at 4 K/min immediately to 25 K, and applying the field after 10 s is indicated by open squares.  $H_{dc}=1$  Oe, Ag(11 at. % Mn).

applied. The subsequent relaxation rate is shown in Fig. 9 for the three different wait times  $t_w=0$  (filled squares), 3600 s (open circles), and 30 000 s (filled circles). For reference purposes the corresponding rate obtained after cooling the sample at 4 K/min directly to 25 K and waiting there 10 s before the field is applied, is included and indicated by open squares. It should also be mentioned that a similar measurement where the sample is directly cooled to 25 K using a cooling rate of 0.25 K/min gives a relaxation rate curve that is closely equal to the curve where a zero second wait time at 23 K is used (filled squares). The prime aging characteristic of the magnetic relaxation in spin glasses is an inflection point in the relaxation rate at an observation time closely equal to the wait time before the magnetic field is applied  $t_w$ . A rather slow cooling rate, such as 0.25 K/min, yields a broad and ill-defined maximum in the relaxation rate at an observation time that may be called effective wait time or

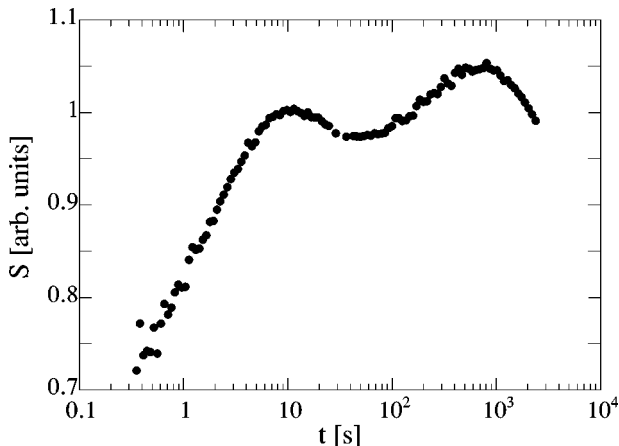


FIG. 10. Relaxation rate  $S$  vs  $\ln t$ , measured at 31 K. The sample was cooled to 31 K, kept there a wait time 1000 s, then cooled to 29.7 K, kept there 3000 s and finally reheated to 31 K, where the dc field was applied.  $H_{dc}=1$  Oe, Ag(11 at. % Mn).

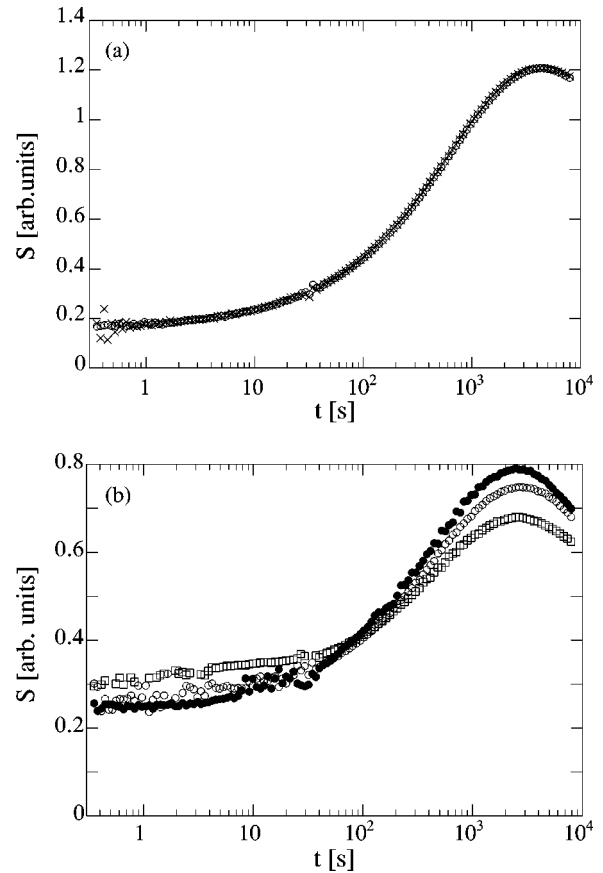


FIG. 11. (a) Relaxation rate  $S$  vs  $\ln t$ , measured at 27 K after a wait time of 3000 s. Crosses: the sample was immediately cooled to 27 K; open circles: the sample was intermittently kept at 31 K for 3000 s during cooling. (b) Relaxation rate  $S$  vs  $\ln t$ , measured at 31 K after having heated the sample back from 27 K and immediately applying the dc field (open squares). Open circles show a corresponding curve where the sample was kept at 23 K for 3000 s instead of at 27 K. Solid circles show the relaxation rate after cooling the sample directly to 31 K and wait 3000 s before applying the field.  $H_{dc}=1$  Oe, Ag(11 at. % Mn).

age. The three curves taken after a cooling rate of 0.25 K/min in Fig. 9 show a continuous development towards the rapidly cooled (4K/min) reference curve with increasing wait time at 23 K. In terms of the droplet model and in agreement with the discussions above, the behavior may be interpreted as follows. A longer wait time at  $T=23$  K should create equilibrated regions on larger and larger length scales, length scales that should approach the typical domain size achieved during cooling at higher temperatures. At 25 K, which on our experimental time scales is out of the overlap region, these regions look random, i.e., with increasing wait time at 23 K, the system should appear more and more reinitialized at  $T=25$  K, just as Fig. 9 shows.

The established way to show the possibility for a spin glass to simultaneously carry several characteristic length scales, at one temperature, is by temperature cycling experiments.<sup>11</sup> The relaxation rate result presented in Fig. 10 is obtained by first cooling the sample to  $T_1=31$  K where it is subjected to a wait time of 1000 s. The temperature is thereafter changed to  $T_2=29.7$  K where it is kept for  $t_{w2}=3000$  s. When returning to  $T_1$  after this temperature cycling, diluted regions of size  $R(T_2, t_{w2})$  have been reinitial-

ized due to the domain wall movements at  $T_2$ . The effect of a third wait time  $t_{w3}=10$  s at  $T_1$  is a system which initially equilibrates in these reinitialized regions up to length scales  $R(T_1, t_{w3})$ . By choosing the temperature step and the wait times carefully it is possible to fulfill the condition  $R(T_1, t_{w3}) < R(T_2, t_{w2}) < R(T_1, t_{w1})$ . The two maxima in the relaxation rate in Fig. 10 then correspond to the nonequilibrium response due to the remaining two relevant characteristic length scales at  $T_1, R(T_1, t_{w3})$  and  $R(T_1, t_{w1})$ .

It is also possible to show that several length scales can coexist in the spin glass at different temperatures with relaxation measurements. Indicated by crosses in Fig. 11(a) is the relaxation rate for the temperature 27 K after a wait time of 3000 s. Also shown in the same figure, indicated by circles, is the relaxation rate after the sample has spent 3000 s at 31 K before the aging at 27 K. No difference in the measured relaxation rate can be resolved between these two procedures. A length scale, caused by the wait time at 31 K is, however, hidden in the second case. In order to reveal this, the sample is heated back to 31 K and immediately probed in a magnetic field. The subsequent relaxation rate is indicated by squares in Fig. 11(b). Also shown by open circles in this figure, is the corresponding relaxation rate but with the second aging at 23 K instead of 27 K. As a reference, the relaxation rate probed directly after the initial wait time at 31 K is shown as filled circles. Basically, all three curves show an age of the system equal to 3000 s only differing in the magnitude of the rate. This experiment, similar to the ac double memory experiment, shows that a spin glass always recalls what has happened during cooling when it is reheated to (or through) the temperature of an interrupted cooling process.

## V. CONCLUSIONS

The nonequilibrium behavior of the dynamic susceptibility of a three-dimensional spin glass has been measured after specific thermal procedures which have been designed to expose certain consequences of a real space spin-glass model including fractal spin-glass domains, droplet excitations, and chaos. A good qualitative agreement between the experimental results and the model predictions is found, which give support for the relevance of droplet scaling pictures to model the dynamics of three-dimensional spin glasses. However, there remain unanswered questions. One crucial point within the model is to obtain an understanding of the difference between the initial fractal domain configuration after a quench and a corresponding snap shot of the equilibrated system with ‘‘active’’ droplet excitations on all length scales. Is it a difference of the fractal dimension of the instantaneous ‘‘domain’’ walls in the two cases that signifies the difference? A prime remaining issue is also to establish if the concept of fractal domains on many length scales can be valid for a model Ising as well as for a real three-dimensional spin glass.

## ACKNOWLEDGMENTS

Financial support from the Swedish Natural Science Research Council (NFR) is acknowledged. Yvonne Andersson and Hui-Ping Liu are acknowledged for invaluable assistance in preparing our AgMn sample.

<sup>1</sup>D. S. Fisher and D. A. Huse, Phys. Rev. B **38**, 373 (1988); **38**, 386 (1988).

<sup>2</sup>L. Lundgren, P. Svedlindh, and O. Beckman, J. Magn. Magn. Mater. **31-34**, 1349 (1983); L. Lundgren, P. Svedlindh, P. Nordblad, and O. Beckman, Phys. Rev. Lett. **51**, 911 (1983).

<sup>3</sup>J. Mattsson, T. Jonsson, P. Nordblad, H. Aruga Katori, and A. Ito, Phys. Rev. Lett. **74**, 4305 (1995).

<sup>4</sup>P. Nordblad and P. Svedlindh, in *Spin-glasses and Random Fields*, edited by A. P. Young (World Scientific, Singapore, 1997).

<sup>5</sup>K. Jonason, E. Vincent, J. Hammann, J. P. Bouchaud, and P.

Nordblad, Phys. Rev. Lett. **81**, 3243 (1998).

<sup>6</sup>J. P. Bouchaud, L. F. Cugliandolo, J. Kurchan, and M. Mezard, in *Spin-glasses and Random Fields* (Ref. 4).

<sup>7</sup>A. J. Bray and M. A. Moore, Phys. Rev. Lett. **58**, 57 (1987).

<sup>8</sup>A. P. Malozemoff and B. Barbara, J. Appl. Phys. **57**, 3410 (1985).

<sup>9</sup>L. Lundgren, P. Svedlindh, and O. Beckman, J. Magn. Magn. Mater. **25**, 33 (1981).

<sup>10</sup>J. Magnusson, C. Djurberg, P. Granberg, and P. Nordblad, Rev. Sci. Instrum. **68**, 3761 (1997).

<sup>11</sup>P. Granberg, L. Lundgren, and P. Nordblad, J. Magn. Magn. Mater. **92**, 228 (1990).